presents a paramagnetic behavior characterized by a Curie constant, $C = 0.55$ for 1 mol of Cu^{2+}, close to the theoretical one ($C_{th} = 0.375$). The large maximum observed above 200 K in the susceptibility curve of CuO disappears, showing that the distance between copper ions is greater in our sample than in CuO. ESR spectra confirm this oxidation degree for copper and show that the copper environment changes by heating the mixture. The shape of the signal indicates that copper is in an axial site. More accurate ESR studies are needed to conclude about the environment, the temperature for which the reaction begins and the quantities of CuO dissolved in the indialite framework.

The solubility of cupric oxide decreases above 1030 °C. Indeed, CuO diffraction lines, missing in the X-ray diffraction pattern of sample $r = 0.25$ heated to 1000 °C, appear again on heating it above 1030 °C. But they are much larger, indicating that the grains, arising from the oxidation of small-sized Cu_2O parallelepipeds on cooling, are much smaller than those of the CuO starting powder. This decrease of copper solubility is probably linked to the reduction of Cu^{2+} to Cu^{+}.

Acknowledgment. We thank J. C. Broudic, I.P.C.M.S. G.M.I. UM 380046, E.H.I.C.S. Strasbourg for supplying indialite sol-gel precursor and helpful discussions, and E. Coronado, Departamento Quimica Inorganica, Facultad Ciencias Quimicas, Burjasot, Spain, for recording ESR spectra.

Registry No. Cu_2O, 1317-39-1; MnO, 1309-48-4; CoO, 1307-96-6; NiO, 1313-99-1; CuO, 1317-38-0; ZnO, 1314-13-2; $Mg_2Al_4Si_5O_{18}$, 12026-18-5; $MgAl_2O_4$, 12068-51-8; Mn_2SiO_4, 13568-32-6; Co_2SiO_4, 13455-33-9; Ni_2SiO_4, 13775-54-7; $ZnAl_2O_4$, 12068-53-0; Zn_2SiO_4, 13597-65-4; SiO_2, 7631-86-9; $MgSiO_3$, 13776-74-4; indialite, 61027-88-1.

Rare-Earth Ions Adsorbed onto Porous Glass: Luminescence as a Characterizing Tool

M. F. Hazenkamp* and G. Blasse

Physics Laboratory, University of Utrecht, P.O. Box 80000, 3508 TA Utrecht, The Netherlands

Received July 24, 1989

The luminescence properties of some rare-earth (Ln) ions adsorbed on porous vycor glass (PVG) are reported. The results are used to characterize this system. Vibronic sidebands of the Gd^{3+} $^6P_{7/2} \rightarrow {}^8S_{7/2}$ emission due to coupling with vibrations of the water molecule and of silica are observed. This observation indicates that the Ln ions are bound to the surface of the pores of PVG and that they are coordinated on the other side by water molecules. From the decay time of Eu^{3+} on PVG, the number of coordinating water molecules is determined by using Horrocks' formula. This number is approximately 4. The energy transfer from Ce^{3+} to Tb^{3+} and from Gd^{3+} to Tb^{3+} is studied. From the dependence of the transfer efficiency on the acceptor concentration, an estimation of the mean distance between two adsorbed in Ln ions is made. This distance is about 7 Å. Ce^{3+} and Eu^{3+} are observed to quench each other's luminescence. The maximum quenching distance is determined to be about 14 Å.

Introduction

Research on the luminescence properties of ions and molecules at solid surfaces is a relatively new subject. Interesting work in this field was done by Anpo et al.,[1] who studied the photoluminescence of heterogeneous catalysts activated with transition-metal complexes. Other work was done on the luminescence of rare-earth ions (with or without an organic complex) adsorbed onto porous vycor glass by Mack and Reisfeld[2,3] and by Blasse et al.[4]

In this paper we present a closer examination of the luminescence properties of some rare-earth ions adsorbed on porous vycor glass. Moreover, we show some cases of interaction between adsorbed rare-earth ions. We will use the results to characterize this system. It was found that luminescence is a suitable tool to provide a qualitative and, to a certain extent, quantitative picture of the structure of the investigated system.

Experimental Section

Sample Preparation. Samples were prepared by impregnating pieces of porous vycor glass (PVG) with aqueous solutions of rare-earth (Ln) ions. The starting materials used were Eu_2O_3, Gd_2O_3, La_2O_3, Tb_4O_7, and $Ce_2(CO_3)_3 \cdot 5H_2O$ (Highways Int. 99.99%). PVG (Corning 7930) is a porous material consisting of 96% SiO_2 and 4% B_2O_3. The internal surface consists of silanol groups. The average pore size is 40 Å, and the BET surface area is about 150 m^2/g.[5] All solutions were prepared by dissolving the Ln salts in hydrochloric acid (Merck P.A.). The concentration of the Ln ions in the solutions was always 0.8 M. By use of this high concentration, the adsorption equilibrium is shifted to the side of the porous glass and the concentration of Ln ions in the pores of PVG is expected to be maximal. When a larger mean distance between the luminescent ions was desired, a part of these ions was replaced by La^{3+} ions. The pH of the impregnating solutions was approximately 0.

Disk-shaped pieces of PVG, 1 mm thick and 10 mm in diameter, were cleaned by boiling for several hours in aqueous 30% H_2O_2

(1) Kubokawa, Y.; Anpo, M. *Adsorption and Catalysis on Oxide Surfaces*; Che, M., Bond, G. C., Eds.; Elsevier Science Publishers: Amsterdam, 1985; p 127.
(2) Mack, H.; Reisfeld, R.; Avnir, D. *Chem. Phys. Lett.* **1983**, *99*, 238.
(3) Reisfeld, R.; Manor, N.; Avnir, D. *Sol. Energy Mater.* **1983**, *8*, 399.
(4) Blasse, G.; Dirksen, G. J.; van der Voort, D.; Sabbatini, N.; Perathoner, S.; Lehn, J.-M.; Alpha, B. *Chem. Phys. Lett.* **1988**, *146*, 347.
(5) Corning technical information.

0897-4756/90/2802-0105$02.50/0

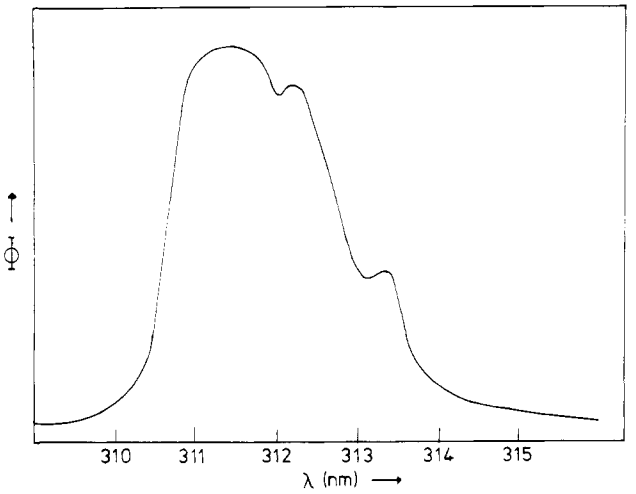

Figure 1. Gd^{3+} $^6P_{7/2} \rightarrow {}^8S_{7/2}$ emission at room temperature of Gd^{3+}/PVG. Excitation is in the Gd^{3+} $^6I_{7/2}$ level at 279.5 nm. Φ gives the spectral radiant power per constant-wavelength interval in arbitrary units.

and stored in deionized water. The pieces, saturated with water of neutral pH, were immersed in the impregnating solution for about 48 h, rinsed with water, and then dried for 2 h at 100 °C in a stream of dry nitrogen. By drying this way, bulk water is removed from the pores while some adsorbed water remains.[6]

After drying, the Ln ions appear only to be present in a thin shell on the outside of the disk. The thickness of this layer was a few tenths of a millimeter. Simultaneous adsorption of Cl^- ions was not checked, but in view of the relatively large concentration of HCl in the impregnating solution, it cannot be ruled out.

Spectroscopic Measurements. The samples were measured immediately after drying. They were kept under nitrogen to avoid extra water adsorption from the atmosphere. Luminescence was measured from the front surface of the disks. All measurements were carried out at room temperature. Low-resolution spectra were recorded by means of a Perkin-Elmer MPF44-b spectrofluorometer. High-resolution spectral and decay measurements were performed on a Quanta Ray Nd:YAG laser setup, as described in ref 7.

Results and Discussion

Gd^{3+} Ion. Upon excitation into the ^6I levels of the Gd^{3+} $4f^7$ configuration at 275 nm, emission lines due to electronic transitions from the Gd^{3+} $^6P_{7/2}$ and $^6P_{5/2}$ levels to the $^8S_{7/2}$ ground level are observed at 311.6 and 306.0 nm, respectively. A high-resolution emission spectrum in the $^6P_{7/2}$ region is presented in Figure 1. The spectrum shows a composite band in which at least three different maxima can be observed. The full width at half-maximum is 220 cm^{-1}.

The $^6P_{7/2}$ emission is considerably broader than that observed for Gd^{3+} in a crystalline host lattice (see, e.g., ref 8). Obviously the Gd^{3+} ions are not precipitated as a crystalline salt in the pores during the drying procedure. The broadening of the $^6P_{7/2}$ emission line is due to the possibility for Gd^{3+} ions to occupy a range of sites at the surface of the pores in the glass in which the Gd^{3+} ion has somewhat different surroundings. This inhomogeneous broadening is also observed when Gd^{3+} or other Ln ions are incorporated into solid glass hosts.[9,10]

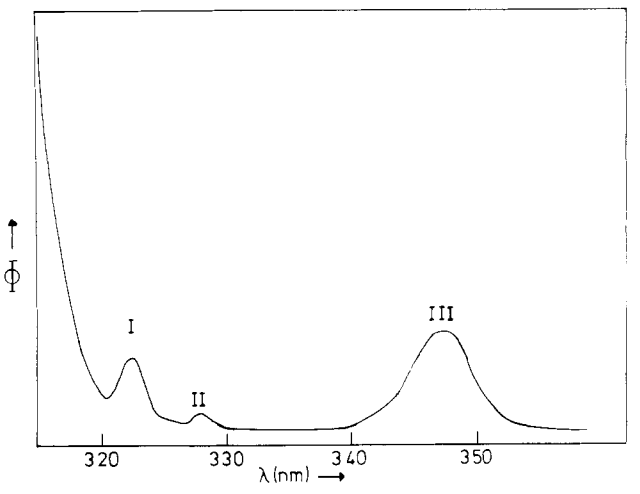

Figure 2. Vibronic side lines of the Gd^{3+} $^6P_{7/2}$ emission at room temperature. See text for the assignment of lines I, II, and III.

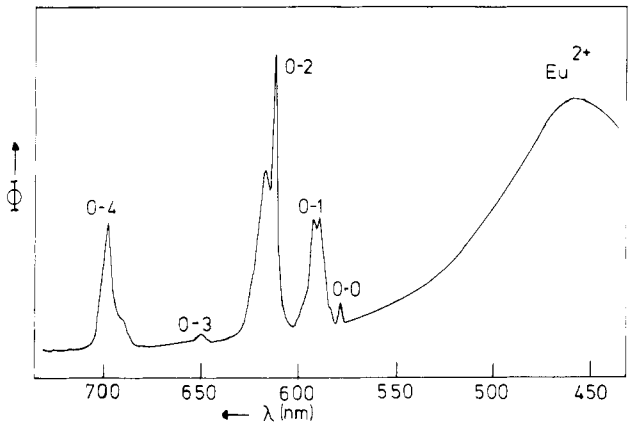

Figure 3. Emission spectrum of Eu^{3+}/PVG. Excitation is at 395 nm. The notation 0-J indicates the transitions $^5D_0 \rightarrow {}^7F_J$.

The three maxima observed in the spectrum of Figure 1 can be ascribed to three different groups of sites at the surface or to different Stark components of the $^6P_{7/2}$ level. The solution of this problem could be the aim for further research.

The emission spectrum at longer wavelengths (see Figure 2) shows three additional lines with intensities of a few percent compared with the $^6P_{7/2} \rightarrow {}^8S_{7/2}$ emission band. These lines, denoted as I, II, and III, are situated at 1090, 1570, and 3280 cm^{-1} lower energy than the maximum of the $^6P_{7/2} \rightarrow {}^8S_{7/2}$ emission line (at 32090 cm^{-1}), respectively. In the emission spectrum of Gd^{3+} in aqueous solution, two additional lines are found with about the same relative positions and intensities as observed for lines II and III.[11]

In ref 11 these lines are attributed to cooperative vibronic transitions involving the OH-bending ($\nu 2$) and OH-stretching ($\nu 3$) vibrations of water molecules coordinating the Gd^{3+} ion. In view of our drying procedure, which does not remove all water from the pores, this assignment is likely to be also valid for lines II and III. In the emission spectrum of Gd^{3+} in aqueous solution there is no line with a relative position and intensity like line I. Line I is therefore most likely due to a cooperative vibronic transition involving the porous glass. In the infrared spectrum of the nonporous Corning borosilicate glass a strong absorption at the same wavenumber (1090 cm^{-1}) as line I is observed.[12] This vibration is due to the

(6) Elmer, T. H.; Chapman, I. D.; Nordberg, M. E. *J. Phys. Chem.* **1962**, *66*, 1517.
(7) de Vries, A. J.; van Vliet, J. P. M.; Blasse, G. *Phys. Status Solidi B* **1988**, *149*, 391.
(8) de Vries, A. J.; Hazenkamp, M. F.; Blasse, G. *J. Lumin.* **1988**, *42*, 275.
(9) Imbusch, G. F. *Phys. Scripta.* **1987**, *T19*, 354.
(10) Verwey, J. W. M.; Imbusch, G. F.; Blasse, G. *J. Phys. Chem. Solids* **1989**, *50*, 813.
(11) Stavola, M.; Friedman, J. M.; Stepnoski, R. A.; Sceats, M. G. *Chem. Phys. Lett.* **1981**, *80*, 192.

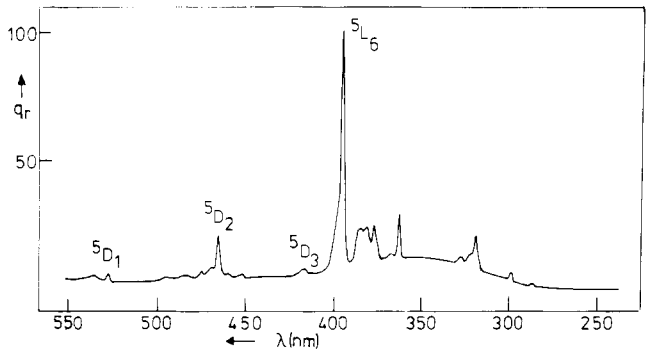

Figure 4. Excitation spectrum of the $^5D_0 \rightarrow {}^7F_2$ emission of Eu^{3+}/PVG. The transitions from the $^7F_0$ level are indicated by the final levels for the lower transitions. q_r gives the relative quantum output.

asymmetrical silicate vibration.

The interaction between an electronic excitation on a Ln ion and a vibronic excitation on another molecule is of a dipole–dipole nature. The strength for this interaction decreases with R^{-6}, which means that only short-range interactions are observed.[11] Therefore, we conclude that the Gd^{3+} ion is bound on one side to the silica surface and on the other side coordinated by water molecules.

It is common that positive ions at surfaces that consist of silanol groups bind ionically to anionic silanol sites.[13,14] It is likely that this is also the case with Ln ions at the surface of PVG.

Eu^{3+} Ion. The emission spectrum of Eu^{3+} adsorbed onto PVG is presented in Figure 3. In this spectrum, the well-known spectral lines due to emission from the Eu^{3+} $^5D_0$ level to the different ^7F ground levels are observed. In addition the spectrum shows a broad emission band at 460 nm. Apart from this broad band the spectrum is essentially the same as the emission spectrum of Eu^{3+} on PVG published by Mack et al.[2] In their interpretation these authors discussed the strong $^5D_0 \rightarrow {}^7F_2$ emission intensity relative to the $^5D_0 \rightarrow {}^7F_1$ emission intensity, which is indicative of Eu^{3+} on low-symmetry sites. Attention should also be given to the relatively strong $^5D_0 \rightarrow {}^7D_0$ emission line, which indicates that the Eu^{3+} ion experiences different chemical coordinations on two sides (a strong linear crystal-field component).[15] This can be understood by considering that the ion is placed at a solid/liquid interface.

The strong broad emission band mentioned above is ascribed to the $4f^65d \rightarrow 4f^7$ transition on Eu^{2+}. The impregnating solution has an absorption band at about 330 nm, which is indicative of Eu^{2+} in aqueous solution.[16] Obviously, a small amount of Eu^{2+} is present in the impregnating solution. Eu^{2+} emission at about the same spectral position (at 445 nm) was observed before in Eu ion-exchanged zeolite Y, in which the exchanged ions are bound to a silica–alumina network.[17] Therefore, we conclude that the Eu^{2+} shows luminescence at room temperature when it is adsorbed onto PVG. The luminescence of Eu^{2+} is, however, completely quenched in aqueous solution.[16] This difference can be explained by assuming that the parabola offset of the excited state of Eu^{2+} is smaller on PVG than in aqueous solution. This means that the Eu^{2+} ion is more tightly bound to its surroundings when it is adsorbed on the silica surface than in aqueous solution.

The excitation spectrum of the Eu^{3+} $^5D_0$ emission is shown in Figure 4. In the spectrum lines due to transitions within the $4f^6$ configuration of Eu^{3+} and a weak broad band between 300 and 420 nm are observed. Excitation into this broad band yields a strong Eu^{2+} emission and must therefore be ascribed to the $4f^7 \rightarrow 4f^65d$ transition on Eu^{2+}. No Eu^{3+} charge-transfer excitation band is observed in the spectral region under investigation (20×10^3 cm$^{-1} < \nu < 40 \times 10^3$ cm^{-1}). The position of the charge-transfer state of Eu^{3+} in aqueous solution is situated above 50×10^3 cm^{-1}.[18] If the Eu^{3+} ion in the porous glass is mainly coordinated by water molecules, the absence of a charge-transfer band below 40×10^3 cm^{-1} is not surprising.

The decay time of the Eu^{3+} $^5D_0$ emission was measured on a sample impregnated with a solution in which 2% of the Ln ions are Eu^{3+} ions and 98% Gd^{3+} ions. This dilution was necessary to prevent Eu^{3+} energy transfer. Excitation was into the Eu^{3+} ions. The decay curve shows a single exponential with a decay time of 0.25 ms. This relatively short lifetime is due to fast nonradiative multiphonon relaxation that involves the OH stretching vibration of the coordinating water molecules. The number of water molecules can be determined by using Horrocks' formula.[19] This formula has proved to be valid for Eu^{3+} in solutions and in (bio)organic complexes in solution. In inorganic solids, however, it should be used with great care as shown by van der Voort et al., who demonstrated that Horrocks' formula cannot be used to determine the number of water molecules coordinating Eu^{3+} in gypsum. This is due to the difference in the coupling strength of the OH vibrations in a solid and in a solution.[20]

The water molecules in the relatively large pores of PVG have considerable freedom to move, comparable to bulk water. It is therefore expected that the Eu^{3+} ion experiences a similar coupling with the OH vibrations as in aqueous solution. Horrocks' formula may therefore be applied in this case. The formula states

$$q(H_2O) = 1.05(1/\tau(H_2O) - 1/\tau(D_2O)) \qquad (1)$$

Here, $q(H_2O)$ is the number of coordinating water molecules, and $\tau(H_2O)$ and $\tau(D_2O)$ are the decay times in H_2O and D_2O coordination in milliseconds, respectively.

A reliable measurement of $\tau(D_2O)$ is rather difficult since PVG is known to be very hygroscopic.[5] A fast exchange of H_2O from the atmosphere for D_2O is expected to occur when a sample is exposed to air. Exposure to wet air cannot be completely avoided. Therefore we employed an indirect procedure to obtain $\tau(D_2O)$.

The value of $1/\tau(D_2O)$ is assumed to be equal to the radiative decay rate of Eu^{3+} in this system. This rate can be estimated from the ratio of the magnetic-dipole emission intensity ($^5D_0 \rightarrow {}^7F_1$) to the total emission intensity from the $^5D_0$ level, since the magnetic-dipole intensity is in good approximation independent of the surroundings. The radiative decay rate of the magnetic-dipole transition can be calculated from the oscillator strength of the $^5D_0 \rightarrow {}^7F_1$ transition determined by Carnall.[18] The decay rate amounts to approximately 50 s^{-1}. The ratio between the

(12) Hunt, J.; Wisherd, M. P.; Bonham, L. C. *Anal. Chem.* **1950**, *22*, 1478.
(13) Shi, W.; Wolfgang, S.; Strekas, T. C.; Gafney, H. D. *J. Phys. Chem.* **1985**, *89*, 974.
(14) Bergaya, B. F.; van Damme, H. *J. Chem. Soc., Faraday Trans. 2* **1983**, *79*, 505.
(15) Blasse, G.; Bril, A. *Philips Res. Rep.* **1966**, *21*, 368.
(16) Sabbatini, N.; Ciano, M.; Dellonte, S.; Bonazzi, A.; Bolletta, F.; Balzani, V. *J. Phys. Chem.* **1984**, *88*, 1534.
(17) Arakawa, T.; Takata, T.; Takakuwa, M.; Adachi, G. Y.; Shiokawa, J. *Mater. Res. Bull.* **1982**, *17*, 171.
(18) Carnall, W. T. *Handbook on the physics and chemistry of rare earths*; Gschneider, Jr., K. A., Eyring, L., Eds.; North Holland: Amsterdam, 1979; Chapter 24.
(19) Horrocks, W. D.; Sudnick, D. R. *Acc. Chem. Res.* **1981**, *14*, 384.
(20) van der Voort, D.; Blasse, G. *Mater. Chem. Phys.* **1989**, *24*, 175.

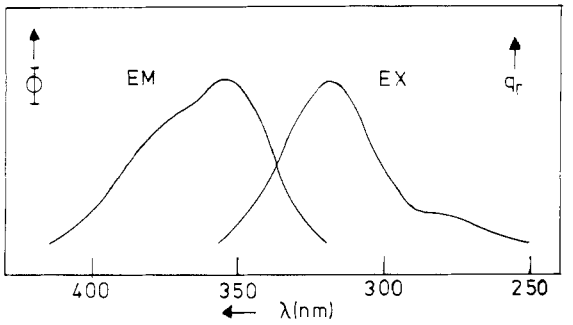

Figure 5. Excitation (right-hand side) and emission (left-hand side) spectra of Ce^{3+}/PVG.

emission intensities was determined from the spectrum in Figure 4 and is about one-sixth. This yields an estimated value of the radiative decay rate of 300 s^{-1}. Applying eq 1 results in $q(H_2O) = 3.9 \pm 1$.

In aqueous solution the Eu^{3+} ion is coordinated by nine water molecules. The lower water coordination found in the present case is due to the fact that the ion is bound to the silica surface on one side and is coordinated by water molecules on the other side, as is also confirmed by the vibronic transitions in the Gd^{3+} emission spectrum. Another confirmation is given in a study by van Damme et al.[14] on Eu^{3+} adsorbed onto mineral clays, which also have a surface consisting of silanol groups. These authors conclude that the Eu^{3+} ion is coordinated by less than eight water molecules. Apart from the coordination by silica oxygen and water, it cannot be excluded that the Eu^{3+} ion is to some extent coordinated by Cl^- ions.

Ce^{3+} Ion. The excitation and emission spectra of Ce^{3+} adsorbed onto PVG are presented in Figure 5. In the excitation spectrum bands at 285 and 320 nm are observed. The transition involved is a 4f → 5d transition. The two bands are ascribed to transitions from the ground level to two different crystal field components of the 5d level. The emission spectrum consist of a broad band situated at 355 nm with a shoulder at about 385 nm, which are ascribed to transitions from the lowest 5d level to the $^2F_{5/2}$ and $^2F_{7/2}$ ground levels of the 4f configuration of Ce^{3+}, respectively. The energy difference between the positions of the shoulder and the band maximum is about 2200 cm^{-1}, and this agrees with values obtained earlier.[22] The doublet structure of the emission band is only weakly revealed due to the inhomogeneous broadening of the emission band.

The Stokes shift determined from the spectra amounts to 3100 cm^{-1}. The Stokes shift of Ce^{3+} in aqueous solution is larger, viz. 5200 cm^{-1}.[21] This difference can be explained by assuming that the parabola offset of the Ce^{3+} 4f → 5d transition is smaller in the case of Ce^{3+} on PVG than in aqueous solution. The same argument was used above to explain the difference in luminescence behavior of Eu^{2+} in these media. In crystalline solids the Stokes shift of Ce^{3+} is often smaller[22] for the same reasons.

Tb^{3+} Ion. The emission spectrum of Tb^{3+} on PVG consists of lines due to transitions from the $^5D_4$ level to the different ^7F_J levels. No emission from higher excited levels is observed. The excitation spectrum of the Tb^{3+} ion on PVG is presented in Figure 6. The spectrum shows lines due to transitions within the $4f^8$ configuration, a band at 265 nm, and the tail of another band, the maximum of which is situated outside the spectral range of the xenon lamp used for excitation. The first band is ascribed to a spin-forbidden $4f^8 \rightarrow 4f^7 5d$ transition. The second band has a much higher intensity and is ascribed to a spin-allowed $4f^8 \rightarrow 4f^7 5d$ transition. The excitation spectrum is essentially the same as the absorption spectrum of Tb^{3+} in aqueous solution published by Carnall.[18]

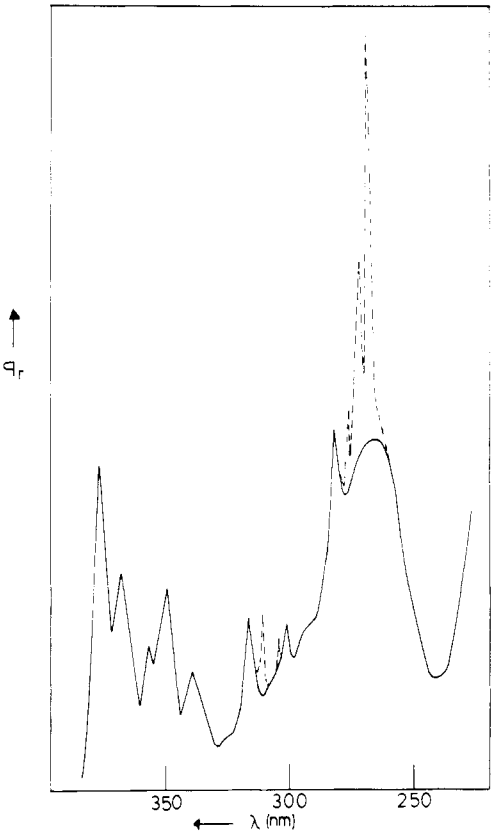

Figure 6. Excitation spectrum of the Tb^{3+} emission of Tb^{3+}/PVG (solid line). The dashed line superimposed on the solid line gives the excitation spectrum of the Tb^{3+} emission of Gd^{3+}/Tb^{3+}/PVG.

Table I. Relative Intensities and *n* Values (See Text) for the Ce^{3+}/Tb^{3+} Experiment

composition of the impregnating soln Ce^{3+}/Tb^{3+}/La^{3+}	$I(Ce^{3+})/I(tot)$	n
0.05/0.025/0.925	0.91	3.7
0.05/0.05/0.90	0.87	2.7
0.05/0.10/0.85	0.72	3.1

Interactions between Adsorbed Ln Ions. A possible interaction between Ln ions adsorbed onto silica surfaces has not been investigated before but is an interesting topic. We investigated three different types of interactions: (a) interaction between Ce^{3+} and Tb^{3+} resulting in energy transfer; (b) interaction between Gd^{3+} and Tb^{3+} resulting in energy transfer; (c) interaction between Ce^{3+} and Eu^{3+} resulting in electron-transfer quenching of the Ce^{3+} emission.

$Ce^{3+} \rightarrow Tb^{3+}$ Energy Transfer. Inspection of Figures 5 and 6 shows that the Ce^{3+} emission band overlaps with some Tb^{3+} excitation lines. If the ions are close enough, energy transfer from Ce^{3+} to Tb^{3+} is expected to occur (see ref 23).

From the Dexter theory the critical radius for energy transfer by dipole–dipole interaction can be calculated from the formula[24,25]

$$R_c^6 = 0.63 \times 10^{28} Q_a E^{-4}(SO) \qquad (2)$$

(21) Svetashev, A. G.; Tsvirko, M. P. *Opt. Spektrosk.* **1984**, *56*(5), 515.
(22) Blasse, G.; Bril, A. *J. Chem. Phys.* **1967**, *47*, 5139.
(23) Blasse, G.; Sabbatini, N. *Mater. Chem. Phys.* **1987**, *16*, 237.
(24) Dexter, D. L. *J. Chem. Phys.* **1953**, *21*, 836.

Here R_c is the critical radius for energy transfer, Q_a the absorption cross section of Tb^{3+}, E the energy at maximum spectral overlap, and SO the spectral overlap. Q_a can be determined from the oscillator strength of Tb^{3+} in aqueous solution as given by Carnall[18] and amounts to 3.5×10^{-21} cm^2 eV. The spectral overlap can be determined from the spectra presented in Figures 5 and 6 and has a value of about 2 eV^{-1}. This results in a R_c value of about 8 Å.

Emission spectra were recorded on samples impregnated with solutions with fixed concentrations of Ce^{3+} and different concentrations of Tb^{3+}. Dilution was done with La^{3+} ions. Excitation at 250 nm yields Ce^{3+} as well as Tb^{3+} emission. Both Ce^{3+} and Tb^{3+} absorb in this region as is clear upon inspection of the excitation spectra. The amount of light directly absorbed by Tb^{3+} can, however, be neglected since the spin-forbidden nature of the involved $4f^8 \rightarrow 4f^75d$ transition accounts for absorptivities that are 2 orders of magnitude lower than those for the involved Ce^{3+} transition.[18] Therefore, practically all Tb^{3+} emission observed is due to energy transfer from Ce^{3+}.

Table I presents the relative intensities of the Ce^{3+} emission for the different samples. The relative Ce^{3+} emission intensity decreases with increasing Tb^{3+} concentration due to energy transfer to Tb^{3+}. This decrease can be described by

$$I(Ce^{3+})/I(\text{tot}) = (1 - x)^n \quad (3)$$

In this formula $I(Ce^{3+})$ is the integrated Ce^{3+} emission intensity and I(tot) the total emission intensity. n is the number of sites around a Ce^{3+} ion to which the Ce^{3+} ion is able to transfer its excitation energy if such a site is occupied by a Tb^{3+} ion. $(1 - x)$ gives the probability that such a site is not occupied by a Tb^{3+} ion.

With this simple formula, the value of n has been calculated for each Tb^{3+} concentration (see Table I). The mean value of n is 3. From the values of R_c and n, the mean distance between neighboring Ln ions can be estimated. We expect that the energy transfer is a two-dimensional process because the ions are adsorbed onto the surface of a pore, the diameter of which is considerably larger than R_c (40 vs 8 Å). We can, therefore, apply the formula

$$l = [(\pi R_c^2)/(n + 1)]^{1/2} \quad (4)$$

where l is the mean distance between neighboring Ln ions. Inserting the values of R_c and n yields a distance l of 7 Å. This distance corresponds to two Ln ions separated by two water molecules.

It should be stressed that this value of l is only an estimate. In determination of the emission intensities two effects were not taken into account: (1) the nonradiative losses on Tb^{3+} due to coupling with OH vibrations of the coordinating water molecules; (2) the energy transfer from Ce^{3+} to killer sites at the glass surface where the excitation energy is lost nonradiatively. These effects decrease the emission intensities of Tb^{3+} and Ce^{3+}, respectively. It may be expected that, to a certain extent, the influence of these two effects cancel each other.

$Gd^{3+} \rightarrow Tb^{3+}$ Energy Transfer. To check the mean separation distance of 7 Å obtained from the Ce^{3+}/Tb^{3+} experiment, the energy transfer from Gd^{3+} to Tb^{3+} was studied. As observed in the excitation spectrum of Tb^{3+} on PVG (Figure 6) the $^6P_{7/2} \rightarrow {}^8S_{7/2}$ emission line of Gd^{3+} (311 nm) overlaps with the $4f^8 \rightarrow 4f^75d$ absorption band of Tb^{3+}. The R_c value for the $Gd^{3+} \rightarrow Tb^{3+}$ energy transfer involving these two transitions can be calculated by using eq 2. Q_a can be determined from the oscillator strengths of the involved transition on Tb^{3+} in aqueous solution and amounts to 5×10^{-20} cm^2 eV.[18] From Figure 6 the spectral overlap is determined, viz., 0.3 eV^{-1}. Inserting these values into eq 2 results in an R_c value of about 8 Å. Efficient energy transfer from Gd^{3+} to Tb^{3+} involving the Gd^{3+} ^6I level is not probable, since the lifetime of this level is expected to be very short due to fast nonradiative relaxation to the ^6P levels.

Table II. Relative Intensities and n Values (See Text) for the Ce^{3+}/Eu^{3+} Experiment

composition of the impregnating soln $Ce^{3+}/Eu^{3+}/La^{3+}$	$I(Ce^{3+})/I(Cd^{3+})_0$	n
0.05/0.05/0.90	0.54	12
0.05/0.10/0.85	0.22	14
0.05/0.20/0.75	0.08	11

Figure 6 presents the excitation spectrum of the Tb^{3+} emission of a sample impregnated with a solution of Gd^{3+} and Tb^{3+} in equal concentrations. The Gd^{3+} absorption lines are clearly observed. The possibility to sensitize the Tb^{3+} emission by Gd^{3+} proves that energy is transfered from Gd^{3+} to Tb^{3+}. This indicates that there are Gd^{3+}–Tb^{3+} pairs within the critical radius (8 Å) from each other, which is confirmed by the average distance between two ions of 7 Å found in the previous paragraph.

Electron-Transfer Quenching of the Ce^{3+} Emission by Interaction with Eu^{3+}. It is known that Ce^{3+} and Eu^{3+} quench each other's luminescence if they are brought together. An excited electron-transfer state (Ce^{4+}/Eu^{2+}) is held responsible for the quenching.[23]

Emission spectra were recorded for samples that contained different amounts of Eu^{3+} and fixed amounts of Ce^{3+}. Table II presents the relative Ce^{3+} emission intensities of the different samples. The Ce^{3+} emission intensity decreases with increasing Eu^{3+} concentration. In the same way as in the Ce^{3+}/Tb^{3+} experiment, this decrease can be described by

$$I(Ce^{3+})/I(Ce^{3+})_0 = (1 - x)^n \quad (5)$$

Here $I(Ce^{3+})_0$ is the Ce^{3+} emission intensity of the sample without Eu^{3+} ions. The other symbols have an equivalent meaning as in the Ce^{3+}/Tb^{3+} experiment.

For every Eu^{3+} concentration, a value of n has been calculated by using this formula (see Table II). The mean value is 12. From the Ce^{3+}/Tb^{3+} experiment it is found that the separation distance between two adsorbed Ln ions, l, is about 7 Å. The quenching of the Ce^{3+} emission is expected to be a two-dimensional process so that the maximum quenching distance, R_q, can be calculated by using the formula

$$R_q = [(n + 1)l^2/\pi]^{1/2} \quad (6)$$

Inserting the values for n and l yields an R_q value of about 14 Å.

From data given in ref 26 it can be calculated that the critical quenching distance between Ce^{3+} and Eu^{3+} in YF_3 is less than 8 Å. Although both values are rather inaccurate, there is no doubt that the quenching distance in PVG is significantly larger than that in YF_3.

This is not unreasonable. The electron-transfer state in the fluoride with less polarizable anions is probably at higher energy than on the PVG. Also, the parabola offset of the electron-transfer state is expected to be larger on the glass than in the crystal. This results in a higher

(25) Blasse, G. *Philips Res. Rep.* **1969**, *24*, 131.

(26) Blasse, G. *Phys. Status Solidi A* **1983**, *75*, 441.

nonradiative rate in the case of the glass (see ref 27).

Conclusions

By investigation of the luminescence properties of Ln ions adsorbed onto the pore surface of PVG it is possible to characterize the chemical structure of this system.

The Ln ions occupy a range of sites with somewhat different chemical surroundings. The ions are bound to the silica surface but are also coordinated by water molecules. The number of water molecules coordinating a Ln ion is approximately four. This water coordination is lower than in aqueous solution (nine coordination) due to the fact that the Ln ion is bound to the silica surface on one side and coordinated by water molecules on the other side.

The adsorbed Ln ions can interact with each other. From the observation of energy transfer from Ce^{3+} to Tb^{3+} and from Gd^{3+} to Tb^{3+} it is found that adsorbed Ln ions are on the average separated about 7 Å from each other. The electron-transfer interaction between Ce^{3+} and Eu^{3+} which is known to exist in the solid state is also observed when the ions are adsorbed onto PVG. A maximum quenching distance of about 14 Å is found.

Acknowledgment. We are indebted to R. van Doorn and Z. Vroon for carrying out part of the experimental work.

Registry No. Gd, 7440-54-2; Eu, 7440-53-1; Ce, 7440-45-1; Tb, 7440-27-9; La, 7439-91-0.

(27) Verwey, J. W. M.; Dirksen, G. J.; Blasse, G. *J. Non-Cryst. Solids* **1988**, *107*, 49.

Influence of Annelation on the Electronic Properties of Phthalocyanine Macrocycles

E. Ortí,* M. C. Piqueras, and R. Crespo

Departamento Química Física, Universidad de Valencia, Dr. Moliner, 50, 46100 Burjassot, Valencia, Spain

J. L. Brédas*

Service de Chimie des Matériaux Nouveaux et Département des Matériaux et Procédés, Université de Mons, Avenue Maistriau, 21, B-7000 Mons, Belgium

Received August 8, 1989

We present the results of valence effective Hamiltonian (VEH) nonempirical pseudopotential calculations on the electronic structure of various macrocycles including tetraazaporphyrin, phthalocyanine, 2,3-naphthalocyanine, 1,2-naphthalocyanine, and phenanthrenocyanine. We focus our attention on the evolution of the oxidation potentials and lowest optical absorptions as a function of linear or angular annelation of benzene rings onto the basic tetraazaporphyrin macrocycle. The VEH results are found to agree with cyclic voltammetry and optical absorption experimental data. These results provide a coherent picture of the evolution of the electrical conductivity properties in crystals and polymers derived from those compounds.

Introduction

Phthalocyanine molecular crystals and cofacially linked polymers are well-documented as materials that may attain high electrical conductivities. Environmentally stable compounds with conductivities on the order of 1–1000 S/cm after partial oxidation by iodine have been reported.[1-3] Although most of the synthetic efforts have been devoted to varying the nature of the atom complexed in the cavity (over 70 different phthalocyanine complexes can be obtained by substituting the central two hydrogen atoms by metal or metalloid atoms), investigations of the transport properties[1-3] indicate that the electrical conductivity has very little dependence on the identity of the complexed atom but is strongly influenced by the orientation and spacing of the phthalocyanine rings. Theoretical studies on the electronic band structures of phthalocyanines[4-8] show that a columnar stacking with minimal spacing leads to an optimal interaction between the π-molecular orbitals on adjacent rings and promotes the highest conductivities. More effective π-interactions and hence higher conductivities could thus be expected if the conjugated system of the phthalocyanine macrocycle becomes more extended. Several synthetic efforts have therefore recently been devoted to obtain crystals and polymers derived from tetraazamacrocycles even larger than phthalocyanine.[9-11]

(1) Marks, T. J. *Science* **1985**, *227*, 881.
(2) (a) Hoffman, B. M.; Ibers, J. A. *Acc. Chem. Res.* **1983**, *16*, 15. (b) Palmer, S. M.; Stanton, J. L.; Martinsen, J.; Ogawa, M. Y.; Hener, W. B.; Van Wallendael, S. E.; Hoffman, B. M.; Ibers, J. A. *Mol. Cryst. Liq. Cryst.* **1985**, *125*, 1.
(3) Hanack, M.; Datz, A.; Fay, R.; Fischer, K.; Keppeler, U.; Koch, J.; Metz, J.; Mezger, M.; Schneider, O.; Schulze, H. J. In *Handbook of Conducting Polymers*; Skotheim, T. A., Ed.; Marcel Dekker: New York, 1986; Vol 1, Chapter 5, p 133.
(4) Whangbo, M.-H.; Stewart, K. R. *Isr. J. Chem.* **1983**, *23*, 133.
(5) Canadell, E.; Alvarez, S. *Inorg. Chem.* **1984**, *23*, 573.
(6) Pietro, W. J.; Marks, T. J.; Ratner, M. A. *J. Am. Chem. Soc.* **1985**, *107*, 5387.
(7) Kutzler, F. W.; Ellis, D. E. *J. Chem. Phys.* **1986**, *84*, 1033.
(8) Gómez-Romero, P.; Lee, Y.-S.; Kertesz, M. *Inorg. Chem.* **1988**, *27*, 3672.
(9) Snow, A. W.; Price, T. R. *Synth. Met.* **1984**, *9*, 329.
(10) Hanack, M.; Renz, G.; Strähle, J.; Schmid, S. *Chem. Ber.* **1988**, *121*, 1479.

0897-4756/90/2802-0110$02.50/0